ASPS Conference Proceedings 1: 999-1005 (2022)

Proceedings of

12th Structural Engineering Convention-An International Event (SEC 2022)

Available at https://asps-journals.com/index.php/acp

Dynamic Analysis for High-Speed Locomotive in Distinct Depths

Engammagari Ganesh [1], Naveen Tiwari [1], Rohit Naharla [1], P.V. Ramana [2,*]

[1] Research Scholar, National Centre for Disaster Mitigation & Management, MNIT Jaipur, India
[2] Professor, National Centre for Disaster Mitigation & Management, MNIT Jaipur, India

Paper ID - 060532

Abstract

The study uses coupled finite or boundary element models expressed in terms of the axial wavenumber. It is found to be important to include the track in the model as this determines how the load is distributed at the soil's surface, which significantly affects the insertion loss of the barrier. Calculations are presented for a range of typical layered grounds in which the depth of the upper soil layer is varied. Variations in the width and depth of the trench or barrier are also considered. The results show that in all ground conditions considered, the notional rectangular open trench performs best.

Keywords: Structural dynamics, Locomotive, Varying depths, Stress analysis.

1. Introduction

From measurements and computer modeling of railway vibration, it has been found that the most important frequency components are controlled by vibration propagation in upper layers of soil that are often only a few meters deep [1,2]. This suggests that a trench that cuts through such a surface layer may potentially give significant reductions in the most important parts of the vibration spectrum. Jones et al. used a two-dimensional boundary element model to study rectangular trenches in the layered ground, considering the effect of their depth and position. The ground consisted of a 2 m layer of alluvial soil over a substratum of stiffer material (say, gravel beds). This study was extended in [3-6] to include trenches with a retaining structure or a slope, again using two-dimensional modeling [7,8].

2. Model

The geometry is essentially two-dimensional and invariant in the third dimension. Under such conditions, it is possible to use a wavenumber transform in the axial direction in combination with a two-dimensional finite or boundary element model [9-12]. The full three-dimensional solution can be recovered by an inverse Fourier transform over wavenumber [13-16]. This so-called 2.5D approach has been used widely to study railway vibration, it is more efficient than a fully dimensional approach. Similarly, 2.5D finite element / infinite element models have been used [17-19].

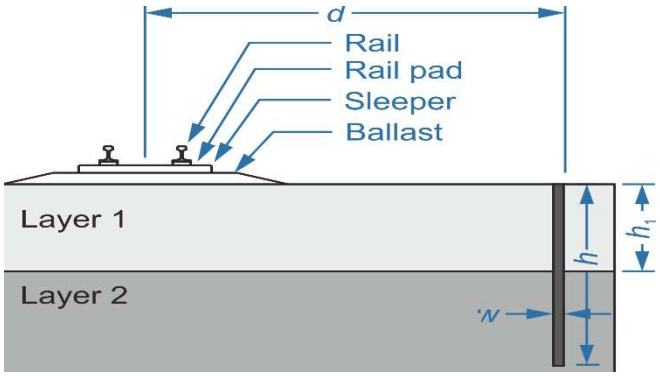

Fig. 1. Layered soil adjacent to a railway track

Table 1: Soil characteristics

	Layer 1	Layer 2
Thickness [m]	0 / 3 / 6 / ∞	∞
Density [kg/m³]	2000	2000
Young's modulus [GN/m²]	0.11	1.8
Poisson's ratio [-]	0.3	0.3
Shear wave speed [m/s]	120	420
Compressional wave speed [m/s]	150	900
Damping loss factor [-]	0.05	0.09

*Corresponding author. Tel: +919549654189; E-mail address: 2021rnc9093@mnit.ac.in

Published online: December 19, 2022
doi:10.38208/acp.v1.612

Table 2: Track Characteristics

Rail	Bending stiffness [MNm²] Mass per unit length [kg/m]	5.8 54.5
Rail pad	Stiffness [MN/m] Damping loss factor [-]	273 0.09
Sleeper	Length [m] Width [m] Height [m] Mass [kg] Young's modulus [GN/m²] Poisson's ratio [-] Sleeper spacing [m]	2.4 0.25 0.20 325 30 0.15 0.60
Ballast	Thickness [m] Shear wave velocity [m/s] Poisson's ratio [-] Density [kg/m³] Damping loss factor [-] Upper width [m] Lower width [m]	0.30 300 1/3 2000 0.04 3.6 5.6

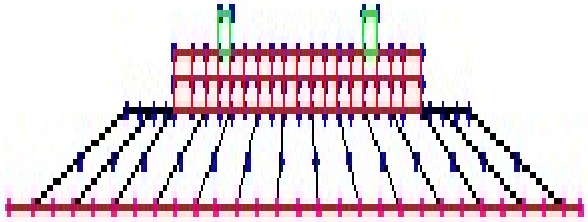

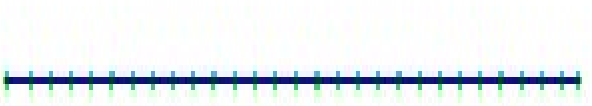

Fig. 2. Layered ground.

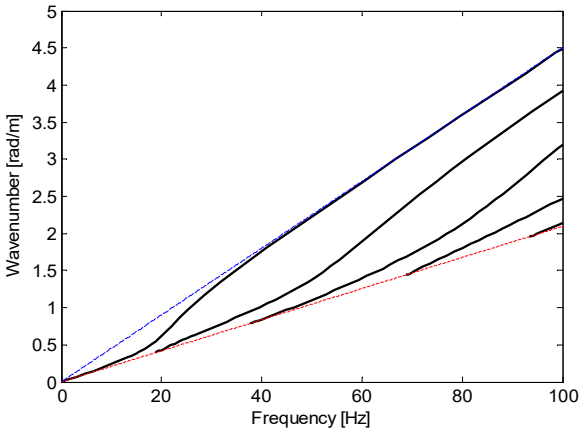

Fig. 3. Dispersion plot

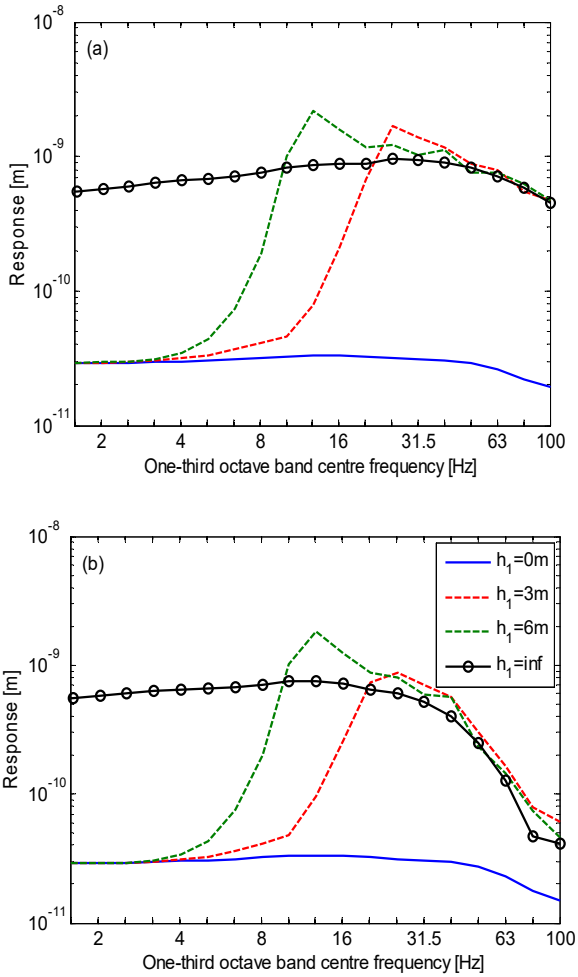

Fig. 4. Response (a) on the ground surface; (b) on the track.

Table 3. Vehicle parameters

Car body mass [kg]	36,000
Car body pitching moment of inertia [kg.m^2]	1.8×10^6
Bogie mass [kg]	4550
Bogie pitching moment of inertia [kg.m^2]	5450
Unsprung wheelset mass [kg]	1600
Total axle load [N]	1.3×10^5
Bogie wheelbase [m]	2.5
Distance between bogie centers [m]	17.3
Overall vehicle length [m]	24.2
Number of vehicles	3.62
Primary suspension stiffness [N/m]	2.2×10^6
Primary suspension viscous damping [Ns/m]	2.3×10^4
Secondary suspension stiffness [N/m]	5.5×10^5
Secondary suspension viscous damping [Ns/m]	1.8×10^4
Contact stiffness (per wheel) [N/m]	1.33×10^9
Train speed [km/h]	228

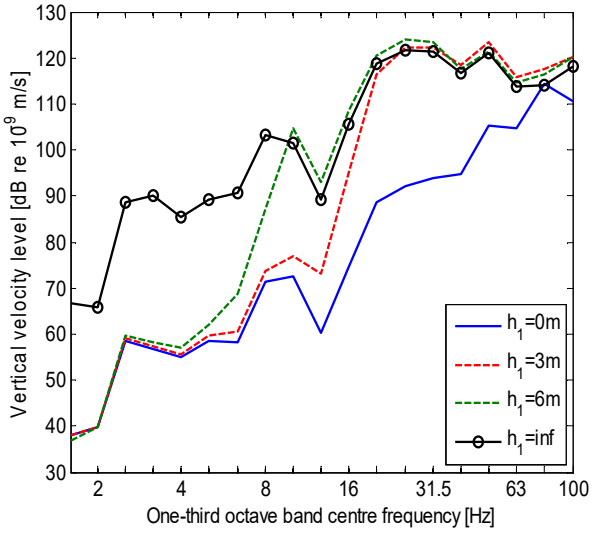

Figure 5: Track for a velocity 250 km/h train.

3. Open Trench

The barrier applies compressional stress to the soil on either side of

$$\sigma = \frac{K_b}{d}(A_1 + A_2 - A_3) \qquad (1)$$

This can be equated to the internal stress in the soil on either side of the barrier

$$\sigma = K_s(-ikA_1 + ikA_2) = -K_s ikA_3 \qquad (2)$$

where $k = \omega/c_p$ is the wavenumber of compressional waves in the soil. Solving these equations yields a power transmission coefficient

$$\tau = \frac{1}{1 + \left(\frac{kK_s d}{K_b}\right)^2} \qquad (3)$$

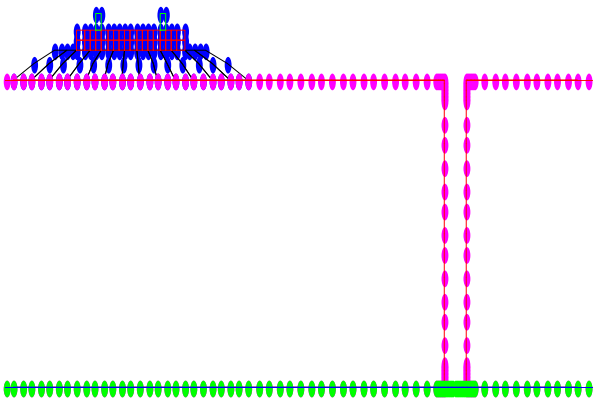

Fig. 6. An open trench

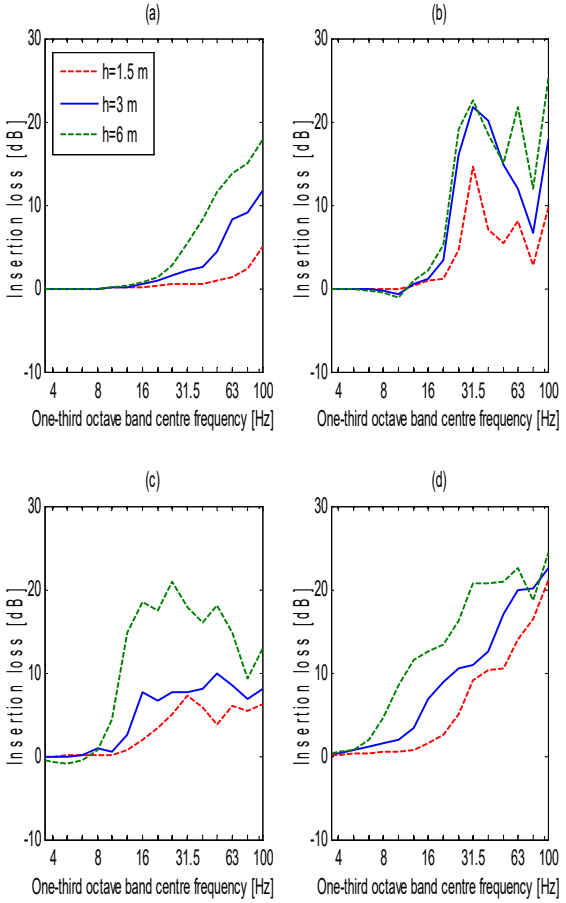

Figure 7: An open trench of varying depths h. (a) h1 = 0 m, (b) h1 = 3 m, (c) h1 = 6 m, and (d) h1 = infinite.

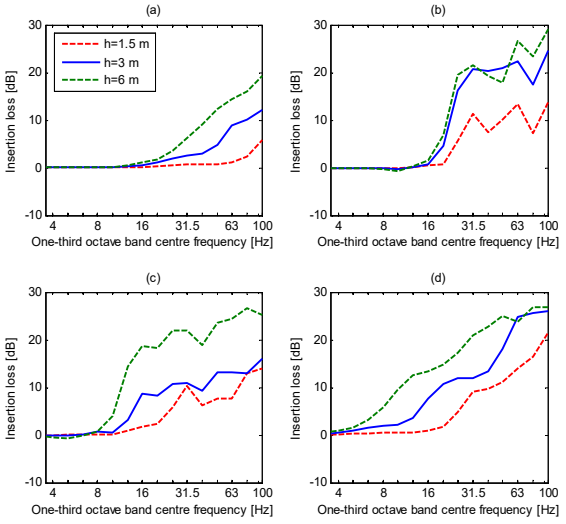

Figure 8: Insertion loss at 24 m from the excitation, with a 0.5 m wide open trench (a) h1 = 0 m, (b) h1 = 3 m, (c) h1 = 6 m, and (d) h1 = infinite.

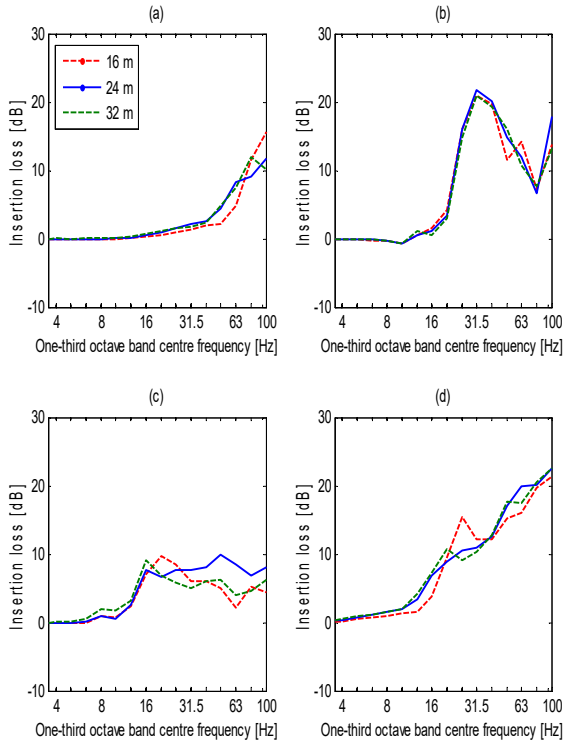

Figure 9: The excitation with a 0.5 m wide open trench of 3 m depth. (a) h1 = 0 m, (b) h1 = 3 m, (c) h1 = 6 m, and (d) h1 = infinite.

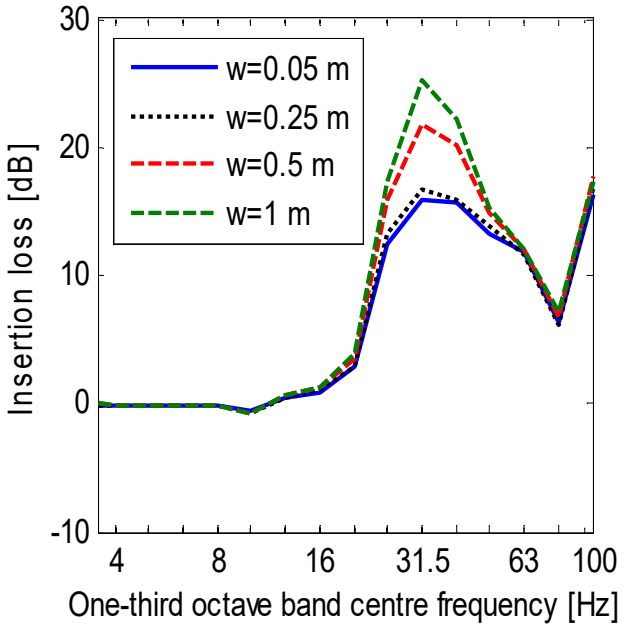

Fig. 10. Effect of varying the width w of a 3 m deep trench on the insertion loss at 24 m, for two-layer ground where the depth of soft upper layer is h_1 = 3 m. Response to a line source; calculated including the track.

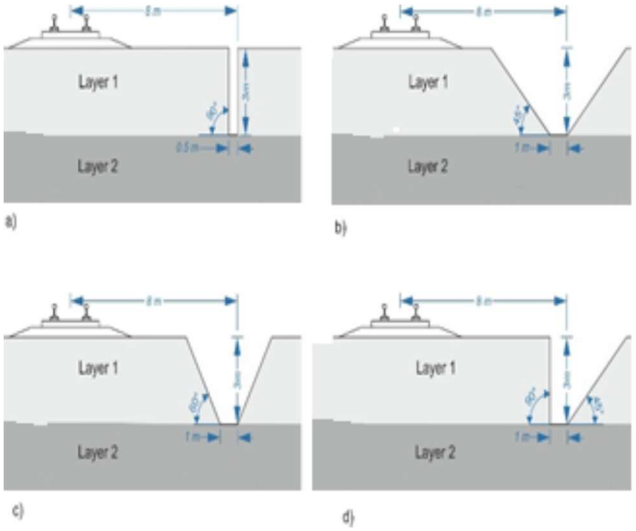

Fig. 11. Trenches with sloping sides

Fig. 12: The angle of the sides of a 3m deep trench on the insertion loss at 24 m with h1 = 3 m soft upper layer depth.

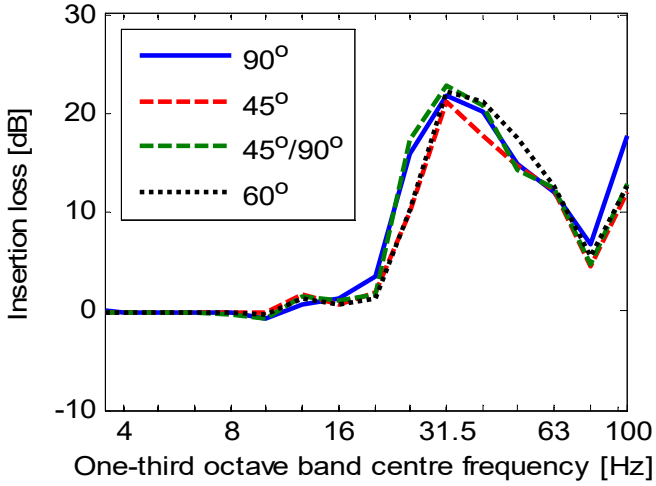

Fig. 12: The angle of the sides of a 3m deep trench on the insertion loss at 24 m with h1 = 3 m soft upper layer depth.

Table 4: The overall velocity levels at 24 m for the passage of traveling at 250 km/h

	h_1 = 0 m	h_1 = 3 m	h_1 = 6 m	h_1 = ∞
No trench	105.9894	117.6246	118.079	116.534
3m trench	98.1720	106.3530	110.9889	105.80
Δ	7.8174	11.2716	7.0902	10.7262
6m trench	92.9907	104.1714	103.3533	100.626
Δ	12.9987	13.4532	14.7258	15.9075

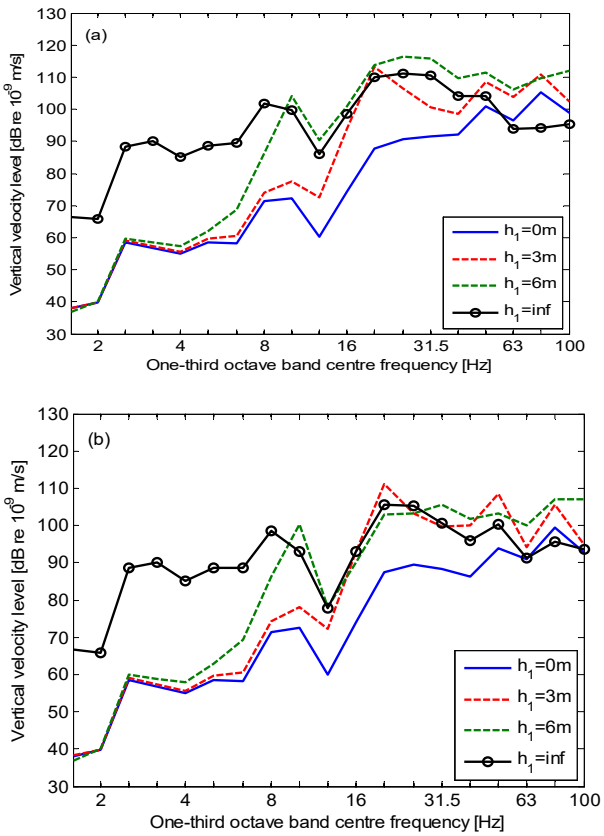

Fig. 13: Vibration caused by passing trains at 24 m from the track for a train speed of 250 km/h and a 0.5 m wide open trench: (a) 3 meters deep; (b) 6 meters deep.

Table 5: Fill material's dynamic properties

	E [MPa]	ν	ρ [kg/m³]	c_s [m/s]	c_p [m/s]	ρc_p [kg/m²s]
A	1.0	0.4	636.3	20.5	50.4	35251
B	0.5	0.4	318.1	20.5	50.4	17625
C	0.25	0.4	159.0	20.5	50.4	8812
D	1.0	0.4	254.5	10.2	25.2	70502
E	0.25	0.4	636.3	10.2	25.2	17625

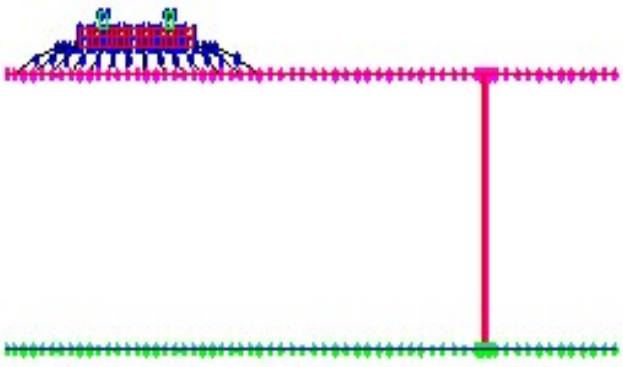

Fig. 14. Geometry of the 2.5D model for buried wall barrier beside a railway track.

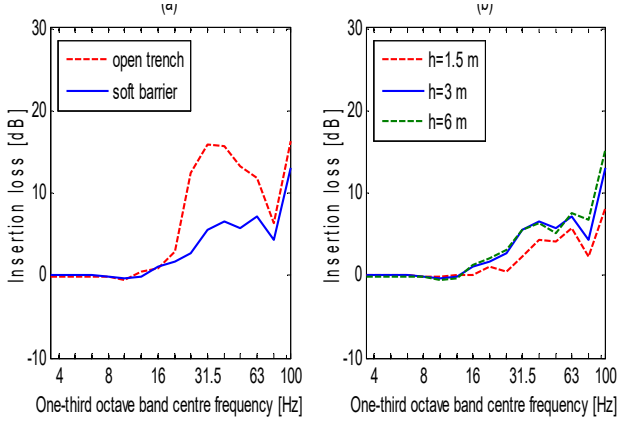

Fig. 15: Insertion loss at 24 m for a 50 mm wide layer depth of h1 = 3 m. (a) Soft barrier 3 m deep versus open trench the same width. (b) Soft barrier with h = 1.5, 3, and 6 m depth. Response to a line source; calculated with the track included.

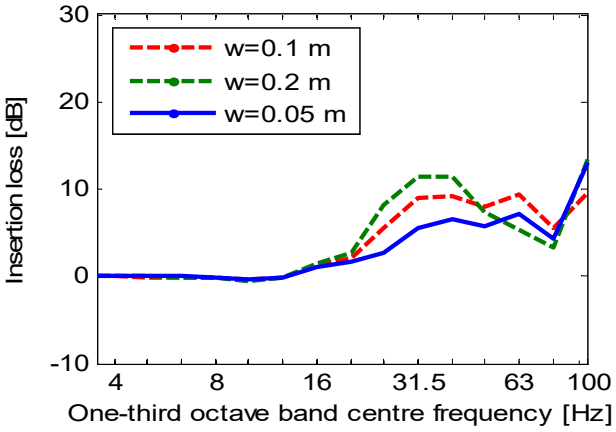

Fig. 16: Insertion loss at 24 m for a 3 m deep soft barrier for a two-layer ground with h1 = 3 m soft upper layer depth.

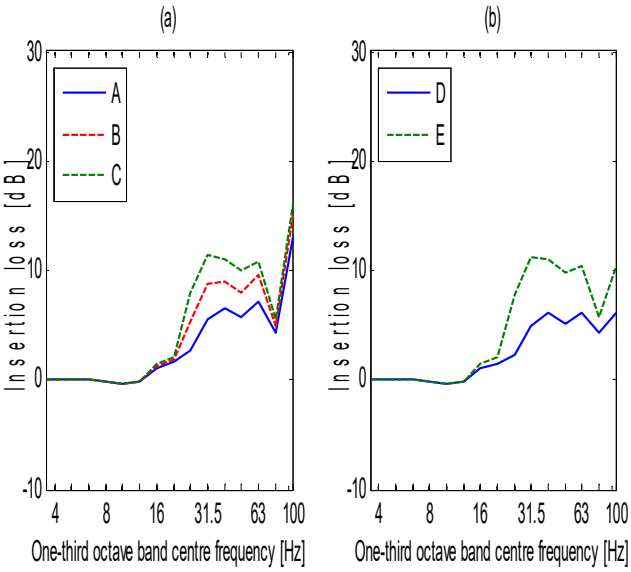

Fig. 16: Insertion loss at 24 m for a 3 m deep soft barrier for a two-layer ground with h1 = 3 m soft upper layer depth.

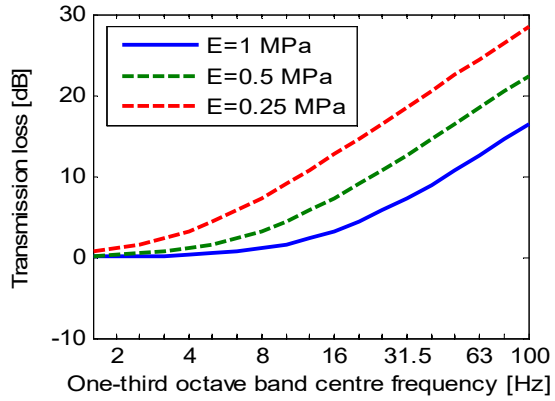

Fig. 17. Transmission loss of an infinite soft-filled barrier with velocity 298 m/s.

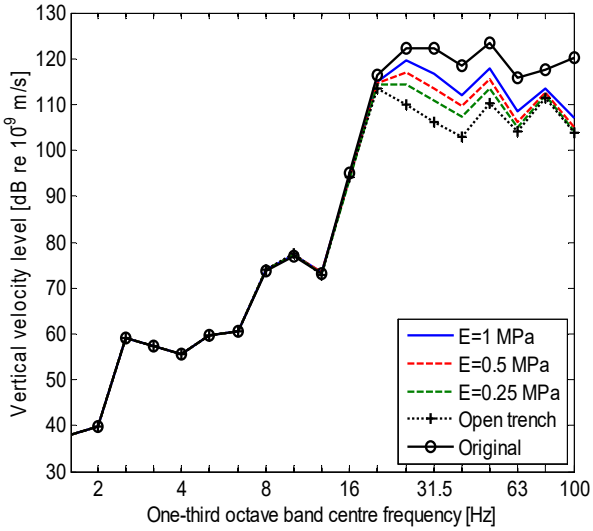

Fig. 18: Predicted vibration due to passing trains at 24 m from the track for a train speed of 250 km/h with a 3 m deep soft-filled barrier, width 0.05 m, and various values of Young's modulus E; two-layer ground with h1 = 3 m soft upper layer depth.

Table 6. Soil properties for the reference sites.

	Layer	h [m]	c_s [m/s]	c_p [m/s]	η [-]	ρ [kg/m³]
Delhi	1	∞	227.3	1336.2	0.0455	1768
Gurugram	1	1.4	116.4	260	0.0800	1636.2
	2	2.7	160	260	0.0691	1636.2
	3	∞	322.7	1515.3	0.0673	1636.2
Faridabad	1	2	140.0	341	0.0455	1636.2
	2	10	108.2	263.6	0.0455	1681.7
	3	∞	181.8	445.4	0.0455	1554.4

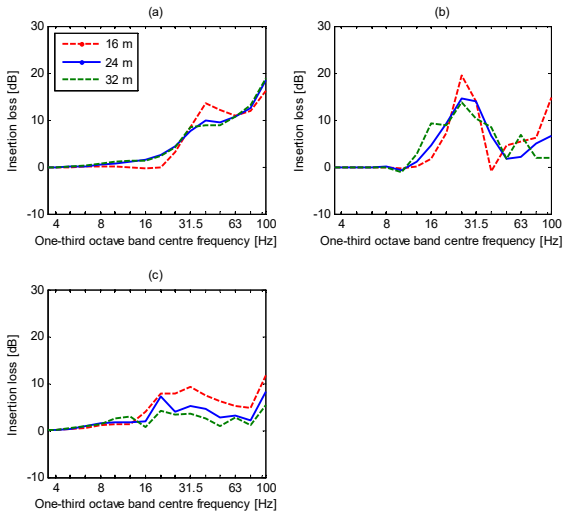

Fig 19: Insertion loss of a 3 m deep, 0.5 m wide open trench for Delhi (a), Gurugram (b), and (c) Faridabad. The receiver is 16 meters (solid line), 24 meters (dashed line), and 32 meters (dash-dot line) away from the track.

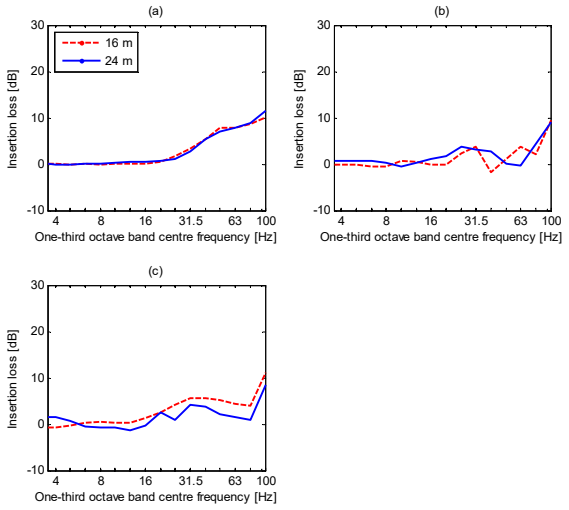

Fig. 20: Insertion loss of a 3 m deep, 50 mm wide soft-filled barrier for different sites. (a) Delhi, (b) Gurugram, (c) Faridabad. The receiver is at 16 m (solid line) and 24 m (dashed line) from the track. Response to a line source; calculated including the track.

4. Conclusions

Filling the trench with a soft barrier material reduces performance significantly because vibration is transmitted through the barrier material and diffracted beneath it. It has been demonstrated that the important parameter is the stiffness per unit area of the barrier material, rather than its impedance, as in the case of transmission at the interface of two semi-infinite media. Despite the reduction in performance, a 3 m deep, 0.05 m wide barrier filled with a material with Young's modulus of 1 MPa reduces overall train-induced vibration by more than 4 dB for the example case considered. This can be improved by reducing the material's stiffness or increasing its width or depth.

Disclosures

Free Access to this article is sponsored by SARL ALPHA CRISTO INDUSTRIAL.

References

1. Ganesh, E., Ramana, P. V., & Shrimali, M. K. (2022). Solved structural dynamic mathematical models via a novel technique approach. Materials Today: Proceedings.
2. Anamika Agnihotri, PV Ramana (2021), Modified Adomian Decomposition Method for Uni-Directional Fracture Problems, Sadhana, unique addition, 1-9.
3. B K Raghu Prasad, P.V. Ramana (2012)," Modified Adomian decomposition method for fracture of laminated uni-directional composites," Sadhana Vol. 37, Part-1, pp.33-57.
4. Ayush Meena, P.V. Ramana (2021), Mathematical Model for Recycled PolyEthylene Terephthalate Material Mechanical Strengths, Materials Today: Proceedings, 38, Part 5.
5. Arigela Surendranath, P.V. Ramana (2021), Mathematical Approach on Recycled Material Strength Performance Via Statistical Mode, Materials Today: Proceedings, 38, Part 5.
6. Ayush Meena, P.V. Ramana (2021), High-Rise Structural Stalling and Drift Effect Owe to Lateral Loading, Materials Today: Proceedings, 38, Part 5.
7. P.V. Ramana (2021), Statistical concert of solid effect on fiber concrete, Materials Today: Proceedings, 38, Part 5.
8. Ganesh, E., Ramana, P. V., & Shrimali, M. K. (2022). Unsolved structural dynamic mathematical models via Novel technique approach. Materials Today: Proceedings.
9. Vivek Singh, P.V. Ramana (2013)," The Magnitude of Linear Problems," "International Conference on Emerging Trends in Engineering & Applied Sciences (ICETEAS)," published in International Journal of Advanced Engineering & Computing Technologies," ISSN: 2249-4928.
10. Ganesh, E., Shrimali, M. K., & Ramana, P. V. (2021). Estimation of Seismic Fragility in Structural Systems. i-Manager's Journal on Structural Engineering, 10(2), 1.
11. Arigela Surendranath, P.V. Ramana (2021), Interpretation of bi-material interface through the mechanical and microstructural possessions Materials Today: Proceedings,17, Part 3.
12. Anamika Agnihotri, P.V. Ramana (2021), Mathematical Model for Recycled PolyEthylene Terephthalate Material Mechanical Strengths, Materials Today: Proceedings, 38, Part 5.
13. Anamika Agnihotri, P.V. Ramana (2021), GGBS: fly-Ash Evaluation and Mechanical properties within high strength concrete, Materials Today: Proceedings, 38, Part 5.
14. Ayush Meena, P.V. Ramana (2021), Assessment of endurance and microstructural properties effect on polypropylene concrete, Materials Today: Proceedings, 38, Part 5.
15. P.V. Ramana (2020), Functioning of bi-material interface intended for polypropylene fiber concrete, Materials Today: Proceedings,14, Part 2.
16. Anamika Agnihotri, P. V. Ramana "Strength and Durability Analysis of GGBS & Recycled Materials," International Conference on Advances in Civil and Structural Engineering (ICACSE-2020), May 28-30, 2020.
17. Ganesh, E., Ramana, P. V., & Shrimali, M. K. (2022). Inelastic materials and mathematical variables for obstacle bridge problem evaluation. Materials Today: Proceedings.
18. A.Wazwaz (1998)," A comparison between Adomian decomposition method and Taylor series method in the series solution", applied mathematics computations, vol.97, pp.37-44.
19. Ganesh, E., Ramana, P., & Shrimali, M. (2022). 3D wave problems evaluation and forecasting through an innovative technique. Materials Today: Proceedings.